

REDUCED-COMPLEXITY POWER AMPLIFIER LINEARIZATION FOR CARRIER AGGREGATION MOBILE TRANSCEIVERS

Mahmoud Abdelaziz¹, Lauri Anttila¹, Abbas Mohammadi², Fadhel Ghannouchi³ and Mikko Valkama¹

¹Department of Electronics and Communications Engineering, Tampere University of Technology, Tampere, Finland

²Department of Electrical Engineering, Amirkabir University of Technology, Tehran, Iran

³Radio Lab, Department of Electrical and Computer Engineering, University of Calgary, Alberta, Canada

E-mails: mahmoud.abdelaziz@tut.fi, lauri.anttila@tut.fi, abm125@aut.ac.ir, fghannou@ucalgary.ca, mikko.e.valkama@tut.fi

ABSTRACT

Spurious intermodulation components have recently been identified as a major problem in carrier aggregation mobile transmitters with multi-band power amplifiers (PAs). This article presents novel adaptive digital predistortion (DPD) solutions with reduced complexity in both the predistortion processing and the feedback paths, to tackle this problem. Compared with conventional DPDs which aim to linearize the whole transmit bandwidth, the proposed technique aims at mitigating only those intermodulation components which are most problematic from the spurious emission limit perspective. The proposed technique is verified with extensive simulations in various 3GPP LTE-A carrier aggregation scenarios, showing that the intermodulation spurs can be efficiently mitigated below the spurious emission limit with relatively small back-offs.

Index Terms— Carrier aggregation, power amplifier, intermodulation, digital predistortion, LTE-Advanced, mobile transmitter

1. INTRODUCTION

One of the major implementation concerns in radio transmitters is the ability to control unwanted spectral emissions. In carrier aggregation (CA) mobile transmitters with a single multi-band power amplifier (PA) [1], some of the intermodulation distortion components created by a nonlinear PA will fall on the spurious region, and may seriously violate the spurious emission limits [2], [3]. To satisfy the stringent emission requirements in such multi-band transmission scenarios, devices may need to considerably back off their transmit power from the nominal maximum value (e.g., +23 dBm in 3GPP LTE uplink). This is called Maximum Power Reduction (MPR) in 3GPP LTE context. However, reducing the transmit power (increasing MPR) in order to fulfill the emission mask will necessarily reduce the uplink coverage. This problem is illustrated e.g. in [3] by showing a measured RF spectrum of an LTE-A Release 12 intraband CA signal with two fully allocated 5 MHz carriers separated by 30 MHz, driving a multi-band PA. The PA nonlinearity creates strong 3rd order spurious intermodulation components at 45 MHz from the center of the whole transmission bandwidth. In this example, more than 11 dB of MPR was needed to keep these intermodulations below the spurious emission limit.

An intriguing alternative solution to power back-off is to use digital predistortion (DPD) linearization for reducing the unwanted

spectral emissions [4–8]. In CA transmit scenarios in battery-powered mobile devices, however, conventional DPDs which take the composite dual-carrier digital signal as input (“full-band DPD”), are not feasible for transmit signal bandwidths exceeding a few tens of MHz, due to the high computational power and sample rate required [5]. In LTE-A with interband CA, for example, the total transmit signal bandwidth can be several hundreds of MHz, thus exemplifying the need for alternative linearization approaches.

In [6], a DPD technique with separate processing for the fundamental bands and the third-order intermodulation (IM3) bands in a dual-carrier transmitter was introduced. This work relied on quasi-memoryless DPD for each subband, and the parameter estimation was non-adaptive, carried out off-line with a large-signal network analyzer (LSNA). In [7], this work was extended to predistort also the fifth-order intermodulation bands with up to three component carriers, still relying on the memoryless modeling and off-line estimation with an LSNA. Memory polynomial based DPD linearization of dual-band PAs, focusing on the spectral regrowth mitigation of the component carriers only, was in turn proposed in [9]. This approach was extended to include also the IM3 bands in [8] but including only memoryless processing. This work represents the current state-of-the-art in the field. The works [6–9] predistort each band separately, thus having much lower sample rate requirements compared to conventional full-band DPDs. In [8] and [9], the DPD parameter estimation is also simplified, since only the linearized bands need to be sampled in the feedback loop. Furthermore, in [6], [7], and [8], the IM3 band distortion compensation is based on injecting a signal with equal magnitude but 180 degree phase shift compared to the estimated IM3 terms, into the input of the transmitter. This approach is here referred to as the 3rd order inverse approach.

In this article, we develop a fully adaptive reduced complexity DPD scheme to specifically target the IM3 bands. In contrast to the previous works in [6], [7], and [8] which utilize the 3rd order inverse solution, we aim to tune the amplitude and phase of the injected signal adaptively, by decorrelating the considered IM3 band signal of the PA output with appropriate basis functions stemming from our analysis and signal modeling. This approach is shown to yield superior results compared to the previous works, while having very low computational and instrumentation complexity. In general, we consider the main objective of the predistorter to keep the spectral emissions below the regulated spectral and spurious emission limits. For the spurious emissions, at RF frequencies over 1 GHz, this limit is -30dBm over a 1 MHz measurement bandwidth [10], [11].

This work was funded by the Finnish Funding Agency for Technology and Innovation (Tekes, under the CREAM project), the Academy of Finland (under the project #251138) and the Austrian Competence Centre in Mechatronics (ACCM).

2. REDUCED-COMPLEXITY DIGITAL PREDISTORTION

2.1. Spurious IM3 Component Modeling and Analysis

In this Section, we first analyze the output of a third-order memoryless PA when excited with a dual-carrier LTE-A UL type signal. A principal scenario illustration is given in Fig. 1. The analysis is carried out at composite baseband equivalent level, and the two component carriers (CC) are assumed to be separated by $2f_{IF}$. Thus, the composite baseband equivalent PA input and output signals, $x(n)$ and $y(n)$, read

$$\begin{aligned} x(n) &= x_1(n)e^{j2\pi\frac{f_{IF}}{f_s}n} + x_2(n)e^{-j2\pi\frac{f_{IF}}{f_s}n} \\ y(n) &= \beta_1x(n) + \beta_3|x(n)|^2x(n) \end{aligned} \quad (1)$$

where β_1 and β_3 are unknown PA coefficients, and $x_1(n)$ and $x_2(n)$ are the baseband equivalents of the input CCs. Through direct substitution of (1) in (2), the baseband equivalent positive and negative IM3 terms, located in the composite BB equivalent at three times the IF frequency, can be easily extracted and read

$$\begin{aligned} y_{IM3+}(n) &= \beta_3(x_2^*(n)x_1^2(n)) \\ y_{IM3-}(n) &= \beta_3(x_1^*(n)x_2^2(n)) \end{aligned} \quad (3)$$

While the PA output contains also other signal and distortion terms, our objective is to develop a low-complexity DPD solution that can in particular reduce the above IM3 components and thus assist the mobile transceiver to fulfill the spurious emission mask with smaller MPR. This is formulated next at structural level in Section 2.2 while the actual parameter optimization and estimation through decorrelation principle are addressed then in Section 3.

2.2. Proposed IM3 Reduction DPD

To simplify the presentation, we focus below on canceling only the $IM3_+$ term in (3). In short, the idea is to inject a proper additional low-power cancellation signal to (1), located at three times the IF, such that $IM3_+$ at PA output is reduced. Stemming from the signal structure in (3), natural injection is of the form $x_2^*(n)x_1^2(n)$ but should be scaled properly with a complex DPD coefficient, say α . Thus, incorporating such DPD processing, the composite baseband equivalent PA input signal reads now

$$\begin{aligned} \tilde{x}(n) &= x_1(n)e^{j2\pi\frac{f_{IF}}{f_s}n} + x_2(n)e^{-j2\pi\frac{f_{IF}}{f_s}n} \\ &+ \alpha(x_2^*(n)x_1^2(n))e^{j2\pi\frac{3f_{IF}}{f_s}n} \end{aligned} \quad (4)$$

Here, and in the continuation, we use $\tilde{(\cdot)}$ variables to indicate DPD-based processing and corresponding signals. Substituting now $\tilde{x}(n)$ in (2), the fundamental CCs and IM3 components at PA output read

$$\begin{aligned} \tilde{y}_+(n) &= \beta_1x_1 + \beta_3|x_1|^2x_1 + 2\beta_3|x_2|^2x_1 \\ &+ 2\beta_3\alpha|x_1|^2|x_2|^2x_1 + 2\beta_3|\alpha|^2|x_1|^4|x_2|^2x_1 \end{aligned} \quad (5)$$

$$\begin{aligned} \tilde{y}_-(n) &= \beta_1x_2 + \beta_3|x_2|^2x_2 + 2\beta_3|x_1|^2x_2 \\ &+ \beta_3\alpha^*|x_1|^4x_2 + 2\beta_3|\alpha|^2|x_1|^2|x_2|^2x_1x_2 \end{aligned} \quad (6)$$

$$\begin{aligned} \tilde{y}_{IM3+}(n) &= (\beta_3 + \beta_1\alpha)x_2^*x_1^2 + 2\beta_3\alpha(|x_1|^2 + |x_2|^2)x_2^*x_1^2 \\ &+ \beta_3|\alpha|^2\alpha|x_1|^4|x_2|^2x_2^*x_1^2 \end{aligned} \quad (7)$$

$$\tilde{y}_{IM3-}(n) = \beta_3x_1^*x_2^2 + 2\beta_3\alpha^*|x_1|^2x_1^*x_2^2 \quad (8)$$

Notice that in above, we have excluded the discrete-time arguments (n) in the signal variables to simplify the presentation. This notational convention is deployed also in the continuation. In addition to above components, the injection of the DPD signal at three times the IF produces then also fifth- and seventh-order IM (IM5 and IM7) terms at the PA output. These are given by

$$\begin{aligned} \tilde{y}_{IM5+}(n) &= \beta_3\alpha^2|x_1|^2x_1^3x_2^{*2} \\ \tilde{y}_{IM5-}(n) &= \beta_3\alpha^*x_1^{*2}x_2^3, \tilde{y}_{IM7+}(n) = \beta_3\alpha^2x_1^4x_2^{*3} \end{aligned} \quad (9)$$

These are, however, typically much weaker than the third-order components which tend to limit the spurious emission performance [10], [11].

As (7) shows, the strength of the considered IM3 at the PA output depends directly on, and can thus be controlled by, the DPD coefficient α . Hence, the optimization and feedback-based low-complexity estimation of α for efficient IM3 cancellation is addressed next in Section 3.

3. DPD PARAMETER OPTIMIZATION AND ESTIMATION

Below we address the DPD parameter optimization and practical estimation. As in the previous Section, we focus mostly on the positive IM3 spurious band to keep the notations compact. Similar processing and optimization can be directly developed then also for the corresponding negative IM3 spurious band. This will also be illustrated in the simulation results section.

3.1. Third-Order Inverse Reference Solution

We start our coefficient optimization by shortly investigating the so-called third-order inverse solution for reference. From (7), it is clear that choosing α such that $\beta_3 + \beta_1\alpha = 0$ or

$$\alpha_{inv} = -\beta_3/\beta_1, \quad (10)$$

the third-order distortion term at positive IM3 band is fully eliminated. This is called here third-order inverse solution. This solution is very intuitive, as injecting $-(\beta_3/\beta_1)x_2^*x_1^2$ at PA input will approximately yield $-\beta_3x_2^*x_1^2$ at the output, thus suppressing the IM3, since the injection is a very low power signal exiting only the PA linear gain. However, as the PA is anyway a fundamentally nonlinear device, some intermodulation will remain at the positive IM3 band. This can be analyzed more closely by substituting $\alpha_{inv} = -\beta_3/\beta_1$ in (7). This yields directly

$$\begin{aligned} \tilde{y}_{IM3+,inv}(n) &= -(\beta_3^2/\beta_1)x_2^*x_1^2[2(|x_1|^2 + |x_2|^2) \\ &+ (|\beta_3|^2/|\beta_1|^2)|x_1|^4|x_2|^2] \end{aligned} \quad (11)$$

Thus we can see that the remaining intermodulation at positive IM3 band contains higher-order terms with structural similarity and correlation with $x_2^*x_1^2$. This will be deployed in Section 3.2 where the proposed decorrelation-based DPD parameter optimization and estimation is formulated. More specifically, denoting the statistical expectation operator by $\mathbf{E}(\cdot)$ and assuming that the CCs x_1 and x_2 are statistically independent, the correlation can be written explicitly as

$$\begin{aligned} \mathbf{E}(\tilde{y}_{IM3+,inv}(n) \times (x_2^*(n)x_1^2(n))^*) &= \\ -\frac{\beta_3^2}{\beta_1} \left[2\mathbf{E}|x_1|^6\mathbf{E}|x_2|^2 + 2\mathbf{E}|x_1|^4\mathbf{E}|x_2|^4 + \frac{|\beta_3|^2}{|\beta_1|^2}\mathbf{E}|x_1|^8\mathbf{E}|x_2|^4 \right] \end{aligned} \quad (12)$$

thus implying non-zero correlation.

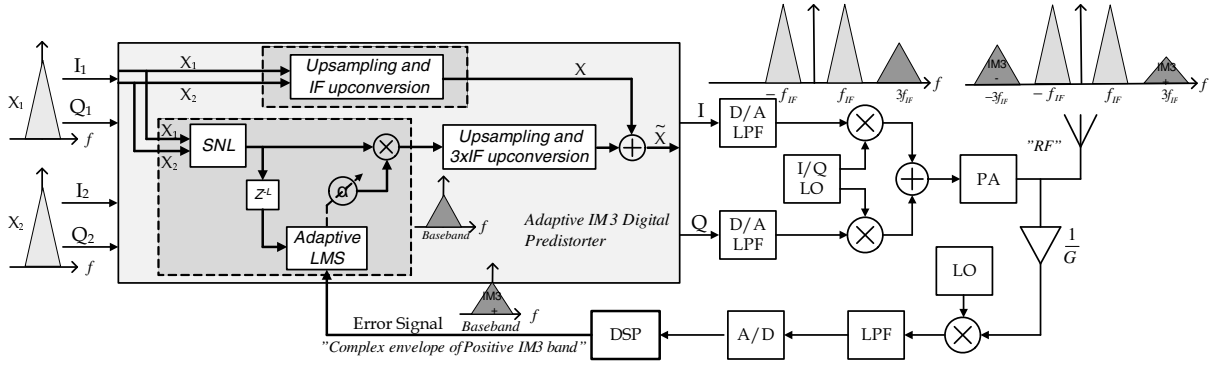


Fig. 1. Principal adaptive DPD system architecture for third-order spurious intermodulation reduction in a dual-carrier transmitter. Also essential composite baseband equivalent spectra are shown.

3.2. Decorrelation-based Parameter Optimization and Practical Adaptive Estimation

As formulated above, the third-order inverse solution in (10) needs explicit estimation of the PA parameters β_1 and β_3 . Furthermore, even with perfect estimation, the remaining distortion has correlation with the essential distortion basis of the form $x_2^*x_1^2$, as was shortly shown above. Hence, opposed to third-order (or more generally P th-order) inverse processing, we formulate the DPD parameter optimization task here as minimizing the correlation between the considered IM3 spurious band and the distortion basis $x_2^*x_1^2$. This will then also imply very simple instrumentation complexity for the feedback receiver, for parameter learning with unknown PA characteristics, as only *narrowband feedback* capturing the considered IM3 spurious band is needed. This is conceptually illustrated in Fig. 1. As formulated in more details below, this will then also enable directly tracking, e.g., possible time-variations in the PA characteristics due to temperature changes and other possible sources like device ageing. Furthermore, very low-complexity practical learning algorithms can be deployed without, e.g., matrix inversion typically encountered in Least-Squares (LS) based block-processing.

We start the mathematical formulation by deploying the *error signal notation*, depicted also in Fig. 1. This error signal, $e(n)$, is defined as the baseband feedback signal from the PA output measured at the considered IM3 spurious band, here the positive one. We also define the cancellation signal basis, also called filter input signal, here as $u(n) = x_2^*(n)x_1^2(n)$ as the focus is on positive IM3 spurious band. We emphasize that this can be generated directly from the baseband signals of the individual component carriers, $x_1(n)$ and $x_2(n)$, at baseband. Then, the idea is find α that minimizes the correlation between $e(n)$ and $u(n)$ and thus orthogonalizes the error signal with the input signal, i.e. sets $E(e(n)u^*(n)) = 0$. To shortly derive this decorrelation solution, we first write the essential instantaneous signal expressions as

$$\begin{aligned} e(n) &= \tilde{y}_{IM3+}(n) \\ &= (\beta_3 + \beta_1\alpha)x_2^*x_1^2 + 2\beta_3\alpha(|x_1|^2 + |x_2|^2)x_2^*x_1^2 \\ &\quad + \beta_3|\alpha|^2\alpha|x_1|^4|x_2|^2x_2^*x_1^2 \end{aligned} \quad (13)$$

$$u(n) = x_2^*(n)x_1^2(n) \quad (14)$$

$$\begin{aligned} e(n)u^*(n) &= \beta_3|x_1|^4|x_2|^2 + \beta_1\alpha|x_1|^4|x_2|^2 \\ &\quad + 2\beta_3\alpha(|x_1|^6|x_2|^2 + |x_1|^4|x_2|^4) + \alpha|\alpha|^2\beta_3|x_1|^8|x_2|^4 \end{aligned} \quad (15)$$

Then, we can directly operate with the statistical expectation operator $E(\cdot)$ to (15), yielding

$$\begin{aligned} E(e(n)u^*(n)) &= \beta_3E|x_1|^4E|x_2|^2 \\ &\quad + \alpha[\beta_1E|x_1|^4E|x_2|^2 + 2\beta_3(E|x_1|^6E|x_2|^2 + E|x_1|^4E|x_2|^4)] \end{aligned} \quad (16)$$

where it has been assumed that the component carrier signals x_1 and x_2 are statistically independent and also the expectation of the last term in (15) has been neglected as it is vanishingly small compared to other terms. Now, setting this expression to zero yields the optimal decorrelating DPD parameter, denoted with α_o , as

$$\alpha_o = \frac{-\beta_3}{\left[\beta_1 + 2\beta_3\left(\frac{E|x_1(n)|^6}{E|x_1(n)|^4} + \frac{E|x_2(n)|^4}{E|x_2(n)|^2}\right)\right]} \quad (17)$$

Interestingly, the derived solution depends on the PA parameters and higher-order statistics of the component carrier signals. As the PA parameters β_1 and β_3 are assumed unknown, this solution cannot be directly evaluated. However, it serves as the reference solution and its derivation also forms directly the basis for developing the actual sample-adaptive practical learning algorithm.

Next, as the PA parameters are assumed unknown, a sample-adaptive or instantaneous decorrelation solution is pursued where only the feedback observation is needed and DPD parameter α is adapted continuously. This can be obtained directly using the instantaneous sample correlation $u(n)e^*(n)$ to update the DPD parameter α . We formulate this as

$$e(n) = \tilde{y}_{IM3+}(n) \quad (18)$$

$$u(n) = x_2^*(n)x_1^2(n) \quad (19)$$

$$\alpha^*(n+1) = \alpha^*(n) - \frac{\mu}{|u(n)|^2}u(n)e^*(n) \quad (20)$$

where learning step-size normalization is also deployed. This resembles closely Normalized Least-Mean-Square (N-LMS) type adaptive filtering but with nonlinear transmitter inside the learning loop, which from the learning perspective is the mapping from DPD injection to IM3 band reference receiver output. In practical implementations, as already depicted in Fig. 1, the delay of the transmitter and feedback receiver chains should also be incorporated in

Table 1. Required MPRs to meet the Spurious Emission Limit with minimum of 95% success rate with different numbers of allocated LTE-A RBs per CC

Number of RBs	MPR, no DPD	MPR, proposed DPD
1	6.4 dB	2.7 dB
10	6.2 dB	2.2 dB
50	4.8 dB	1.5 dB

the learning recursion. This type of learning algorithm can also be interpreted as a stochastic Newton root search in the function $J(\alpha) = \mathbf{E}[u(n)e^*(n)]$ (i.e., (16)), with the inverse of the gradient of $J(\alpha)$ approximated with the (positive) scalar $\mu/|u(n)|^2$. This is plausible since the gradient of (16) is indeed positive when the PA total output signal is still dominated by linear signal terms.

4. SIMULATION RESULTS AND ANALYSIS

A dual-carrier LTE-A UL SC-FDMA signal is deployed to test and demonstrate the proposed DPD concept. The CCs are separated by 60 MHz and 25 resource blocks (RB) are allocated at each CC deploying QPSK subcarrier modulation. The IIP3 of the 3rd-order PA model is 17 dBm and the PA output power is +21dBm. As can be seen in Fig. 2, the proposed decorrelation-based DPD provides better results compared to the 3rd-order inverse solution, even when the sample-adaptive practical learning is deployed. Fig. 3 shows the corresponding convergence of the DPD coefficient, together with the derived optimum value α_0 .

For more realistic performance assessment, a 5th-order PA model is next deployed while still carrying out the linearization with IM3 emphasis and sample-adaptive decorrelation-based learning. Furthermore, both IM3+ and IM3- bands are linearized implying parallel learning and processing with separate coefficients, say α_+ and α_- . The results in terms of transmitter output spectra are illustrated in Fig. 4. Clearly, the existence of 5th-order terms have certain impact on the linearization performance but the transmitter emission requirements are still fulfilled with +22dBm output power. To address shortly the impact of 5th-order distortion at IM3 band, and assuming a polynomial PA model of the form $y(n) = \beta_1 x(n) + \beta_3 |x(n)|^2 x(n) + \beta_5 |x(n)|^4 x(n)$, one can easily show that without DPD processing, the positive IM3 band baseband equivalent observation is equal to $\beta_3 (x_2^* x_1^2) + 3\beta_5 |x_2|^2 (x_2^* x_1^2) + 2\beta_5 |x_1|^2 (x_2^* x_1^2)$. Thus, the IM3 bands contain additional signal terms, due to 5th-order distortion in the PA. Compared to the 3rd-order term, these terms are clearly correlated and thus have an impact on the pre-distortion coefficient learning. Extending the pre-distortion processing to adaptively decorrelate the higher-order distortion terms at IM3 bands is thus an important topic for future work.

Finally, we elaborate on the ability of the developed DPD solution to relax the MPR requirements in different RB allocation scenarios, using the 5th-order PA model. Table 1 shows the required MPRs, without and with DPD, in order to ensure meeting the spurious emission mask defined in [10] and [11] in large number of parallel realizations with at least 95% success rate. It is evident that the proposed DPD allows using lower MPRs, by at least 3-4 dB, depending on the number of allocated RBs. This directly reflects on the UL network coverage.

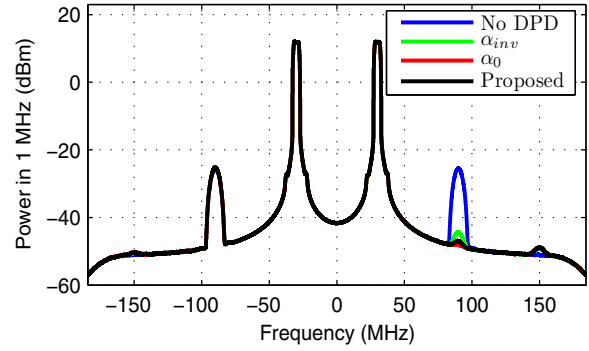


Fig. 2. Dual-carrier LTE-A mobile transmitter power spectra without and with DPDs. PA with 17 dBm IIP3 and output power of +21 dBm.

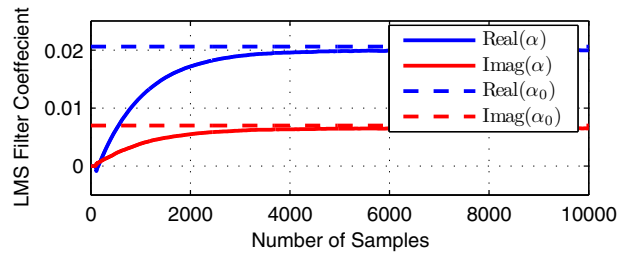


Fig. 3. Illustration of sample-adaptive decorrelation coefficient convergence and the corresponding optimum coefficient.

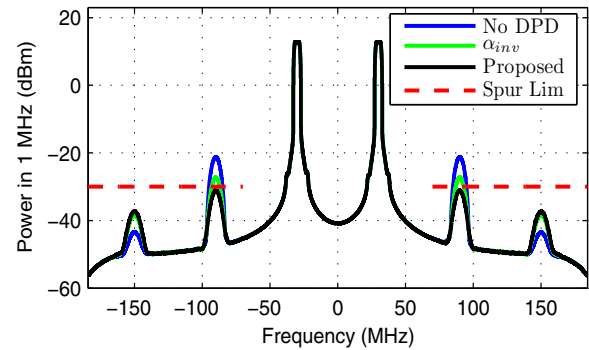


Fig. 4. Dual-carrier LTE-A mobile transmitter power spectra without and with DPD. 5th-order PA model having 1-dB compression point of 26 dBm and output power of +22 dBm.

5. CONCLUSIONS

In this paper, reduced-complexity adaptive digital pre-distortion solution was developed to specifically suppress third-order intermodulation in non-contiguous dual-carrier mobile transmitters. Sample-adaptive parameter learning algorithm deploying only narrowband feedback was formulated, and the whole DPD concept was shown to outperform the existing third-order inverse solutions. This can help dual-carrier mobile devices to reduce their power back-off while still fulfilling the spurious emission requirements. Future work will include extending the DPD processing and parameter learning to high-order PAs with memory.

6. REFERENCES

- [1] S.A. Bassam, Wenhua Chen, M. Helou, and F.M. Ghannouchi, "Transmitter architecture for CA: Carrier Aggregation in LTE-Advanced systems," *IEEE Microwave Magazine*, vol. 14, 2013.
- [2] V. Lehtinen, T. Lähteensuo, P. Vasenkari, A. Piipponen, and M. Valkama, "Gating factor analysis of maximum power reduction in multicarrier LTE-A uplink transmission," in *Proc. IEEE Radio and Wireless Symposium (RWS)*, Austin, TX, Jan. 2013.
- [3] T. Lähteensuo, "Linearity requirements in LTE Advanced mobile transmitter," M.S. thesis, Tampere University of Technology, Tampere, Finland., May 2013. <http://dspace.cc.tut.fi/dpub/handle/123456789/21504>.
- [4] J. Thorebäck, "Digital predistortion the evolution of linearized transmitters for radio basestations," in *Signal Processing for Amplifiers Workshop, Chalmers, Sweden*, Nov. 2012.
- [5] M. Abdelaziz et al., "Mobile transmitter digital predistortion: Feasibility analysis, algorithms and design exploration," in *47th Asilomar Conf. Signals Systems Computers, Pacific Grove, CA, USA*, Nov. 2013.
- [6] P. Roblin, S. K. Myoung, D. Chaillot, Y. G. Kim, A. Fathimulla, J. Strahler, and S. Bibyk, "Frequency-selective predistortion linearization of RF power amplifiers," *IEEE Transactions on Microwave Theory and Techniques*, vol. 56, pp. 65–76, Jan. 2008.
- [7] J. Kim, P. Roblin, D. Chaillot, and Z. Xie, "A generalized architecture for the frequency-selective digital predistortion linearization technique," *IEEE Transactions on Microwave Theory and Techniques*, vol. 61, pp. 596–605, Jan. 2013.
- [8] S.A. Bassam, M. Helou, and F.M. Ghannouchi, "Channel-selective multi-carrier digital predistorter for multi-carrier transmitters," *IEEE Transactions on Microwave Theory and Techniques*, vol. 60, pp. 2344–2352, Aug. 2012.
- [9] S.A. Bassam, M. Helou, and F.M. Ghannouchi, "2-D Digital Predistortion (2-D-DPD) architecture for concurrent dual-band transmitters," *IEEE Transactions on Microwave Theory and Techniques*, vol. 59, pp. 2547–2553, Oct. 2011.
- [10] "3GPP Evolved Universal Terrestrial Radio Access (E-UTRA); User Equipment (UE) radio transmission and reception. <http://www.3gpp.org/ftp/specs/html-info/36101.htm>," .
- [11] "International telecommunication union radio communication sector, recommendation ITU-R SM.329-12 unwanted emissions in the spurious domain. http://www.itu.int/dms_pubrec/itu-rec/sm/R-REC-SM.329-12-201209-i!!PDF-E.pdf," .